INSTITUT DES SCIENCES ET TECHNOLOGIES
PARIS INSTITUTE OF TECHNOLOGY

École doctorale n° 364 : Sciences Fondamentales et Appliquées

Doctorat ParisTech

THÈSE

pour obtenir le grade de docteur délivré par

l'École Nationale Supérieure des Mines de Paris

Spécialité doctorale "Science et Génie des Matériaux"

présentée et soutenue publiquement par

Ali Saad

le xx juin 2015

Numerical Modelling of Macrosegregation Formed During Solidification With Shrinkage Using a Level Set Approach

Directeurs de thèse: **Michel Bellet**
Charles-André Gandin

Jury

M. Blablabla,	Professeur, MINES ParisTech	Rapporteur
M. Blablabla,	Professeur, Arts Et Métiers ParisTech	Rapporteur
M. Blablabla,	Chargé de recherche, ENS Cachan	Examinateur
M. Blablabla,	Danseuse, en freelance	Examinateur
M. Blablabla,	Ingénieur, MIT	Examinateur

MINES ParisTech
Centre de Mise en Forme des Matériaux (CEMEF)
UMR CNRS 7635, F-06904 Sophia Antipolis, France

T H E S E

Contents

Acronym	Standing for
ALE	Arbitrary Lagrangian-Eulerian
BTR	Brittleness temperature range
CAFD	Cellular Automata Finite Difference
CAFE	Cellular Automata Finite Element
CBB	Circumventing Babuška-Brezzi
CCEMLCC	Chill Cooling for the Electro-Magnetic Levitator in relation with Continuous Casting of steel
CEMEF	Center for Material Forming
CSF	Continuum Surface Force
DLR	Deutsches Zentrum für Luft- und Raumfahrt
EML	Electromagnetic levitation
ESA	European Space Agency
FEM	Finite Element Method
GMAW	Gas Metal Arc Welding
ISS	International Space Station
IWT	Institut für Werkstofftechnik
LHS	Left Hand Side
LSM	Level set method
MAC	Marker-and-cell
PF	Phase field
RHS	Right Hand Side
RUB	Ruhr Universität Bochum
RVE	Representative Elementary Volume
SBB	Satisfying Babuška-Brezzi
SCPG	Shock Capturing Petrov-Galerkin
SUPG	Streamline Upwind Petrov-Galerkin
VMS	Variational MultiScale
VOF	Volume Of Fluid

Chapter 1

Macrosegregation with solidification shrinkage

Contents

1.1 Solidification shrinkage

Solidification shrinkage is, by definition, the effect of relative density change between the liquid and solid phases. In general, it results in a progressive volume change during solidification, until the phase change has finished. The four stages in figs. 1.1a to 1.1d depict the volume change with respect to solidification time. First, at the level of the first solid crust, near the local solidus temperature, the solid forms with a density greater than the liquid's. The subsequent volume decrease creates voids with a negative pressure, forcing the fluid to be sucked in the direction of the volume change (cf. fig. 1.1b). As a direct result of the inward feeding flow, the ingot surface tends to gradually deform in the feeding direction, forming the so-called *shrinkage pipe*, shown in fig. 1.2. Since the mass of the alloy and its chemical species is conserved, a density difference between the phases ($\rho^l < \rho^s \implies \frac{\rho^l}{\rho^s} < 1$) eventually leads to a different overall volume ($V^s < V^l$) once solidification is complete, as confirm the following equations:

$$\rho^l V^l = \rho^s V^s \tag{1.1a}$$

$$V^s = \frac{\rho^l}{\rho^s} V^l \tag{1.1b}$$

Solidification shrinkage is not the only factor responsible for volume decrease. Thermal shrinkage in both solid and liquid phases, as well as solutal shrinkage in the liquid phase are also common causes in a casting process. However, thermal shrinkage is very important to apprehend, as temperature decreases in steel casting, usually exceeding a 1000 °C, thus causing substantial density variations.

1.2 Choice of interface tracking

In chapter 2, several methods of interface tracking/capturing methods were presented along with their similarities and differences. In the case of solidification shrinkage, the metal-air interface can be tracked with any method from the previously mentioned. However, several reasons motivate us to settle on the level set method. First, the easiest solution is testing a method which already exists in *CimLib* library. The level set method was implemented by HERE as a framework for monolithic resolution. Since this work, the method has been extensively used and improved in several projects mainly for multiphase flows, which is the main competence of the Computational Fluids LXXXX group at CEMEF. Another motivation is the compatibility between *CimLib* and *Thercast*®, where the latter is the final destination of the code developed during for the Ph.D. thesis. In its recent versions, *Thercast*® handles laminar and turbulent ingot filling where the level set method is used to capture the free surface of the molten metal. Aside from the practical motivations, some technical aspects of

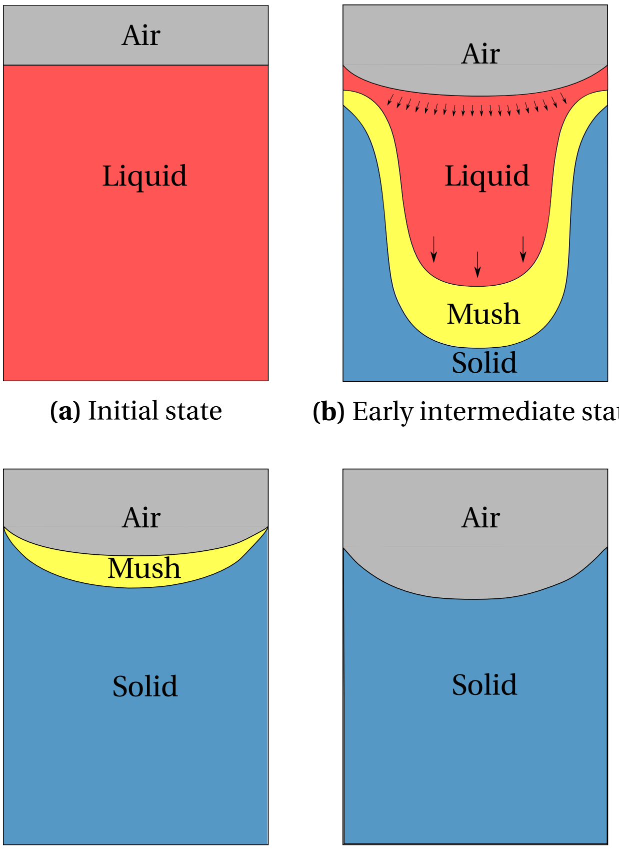

(a) Initial state

(b) Early intermediate state

(c) Late intermediate state

(d) Final state

Fig. 1.1 – Schematic of the main cooling stages of an ingot against side and bottom mould walls (not shown)

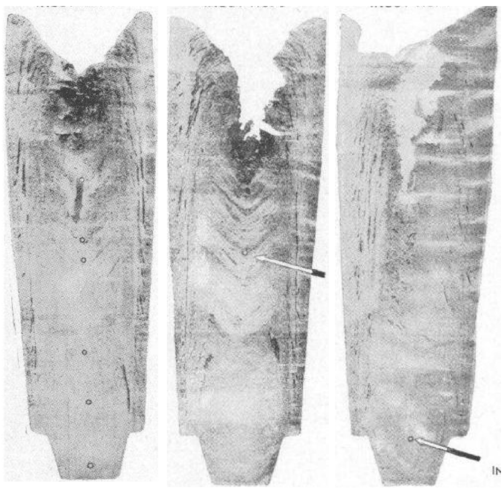

Fig. 1.2 – Sulphur prints of three ingots showing pipe formation at the top as a result of solidification shrinkage with various ingot inclination during casting [Onodera et al. 1959]. Positive macrosegregation is clearly seen in this area, while A-shape and V-shape positive mesosegregates are detected at the ingot's tips and center respectively.

the level set method make it very attractive to apply it macroscopic surface tracking (in contrast to microscopic interface tracking, for instance the solid-liquid interface), such as topological properties that are readily available (e.g. curvature) and accurate position compared to volume-based methods like VOF.

1.3 Multidomain formalism

In the previous chapters, we considered in our simulations the metal as a saturated mixture of solid and liquid during solidification. It means that no gas phase may appear during the process, and this this chapter. The reason is we chose to describe our model in Eulerian description, for which we have considered a fixed grid to discretise the averaged conservation equations governing the phase change between the liquid and solid phases. Furthermore, with the introduction of shrinkage, an increase in global density means that a gas phase should enter the domain to replace the shrunk volume. At this point, several interfaces may be distinguished: liquid-solid (l-s), liquid-air (l-a) and solid-air (s-a), where we defined 2 phases (l and s) belonging to the "Metal" domain denoted M, while the "Air" domain, denoted A, is made up of a unique phase, (a), with the same name. As a standard for this formalism, we consider that uppercase letters are used for domains, while lowercase letters are used for phases.
The main idea behind the multidomain formalism, is to go from the classic conservations equations introduced by volume averaging in chapter 2, in the context of a solidifying two-phase system to generalise it by taking into account a third gas phase, such as:

$$V^l + V^s + V^a = V_{\mathrm{E}} \tag{1.2}$$

$$g^l + g^s + g^a = 1 \tag{1.3}$$

while keeping a physical integrity with the former monodomain model. Then, one is free to choose a suitable numerical method to track the interfaces between the several phases. In our applications, we are particularly interested in keeping an indirect representation of the l-s interface (dotted line in fig. 1.3) using the volume averaging theory, while employing a different method to track the l-a and s-a interfaces (dashed lines in fig. 1.3) with the level set method. This allows switching to the latter method in a physically representative manner.
In this context, each domain can be seen as a material having a physical interface with the other domains. As a consequence of our interpretation, the gas phase should not exist in the metal, which may naturally occur if the thermodynamic conditions are in favour of nucleating and growing a new phase, or in the case of a gas that was trapped inside mould grooves.

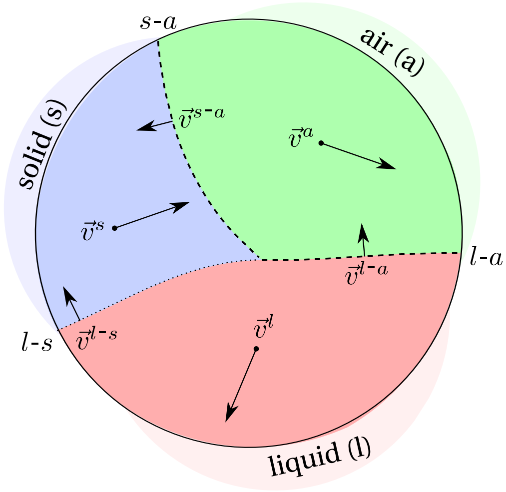

Fig. 1.3 – Schematic of a representative volume element containing 3 phases with distinct velocities, separated by 3 interfaces. The dotted line is the indirectly tracked solid-liquid interface while the other dashed lines, air-liquid and air-solid interfaces, are directly tracked.

1.3.1 Assumptions

Each phase in the system has its own velocity, $\overrightarrow{v^l}$, $\overrightarrow{v^s}$ and $\overrightarrow{v^a}$, while the respective interfaces l-s, l-a and s-a have different and independent velocities, represented by $\overrightarrow{v^{l\text{-}s}}$, $\overrightarrow{v^{l\text{-}a}}$ and $\overrightarrow{v^{s\text{-}a}}$. Note that the solid-liquid interface velocity was denoted $\overrightarrow{v^*}$ in the previous chapters as no more than two phases were considered. The first major assumption is that the solid phase, once formed from the liquid, is fixed and rigid. It means that no subsequent deformation may occur and therefore $\overrightarrow{v^{s\text{-}a}}$ reduces to vector zero. Moreover, we use the already introduced volume averaging principles to write locally for any quantity ψ:

$$\langle \psi \rangle = \left\langle \psi^l \right\rangle + \langle \psi^s \rangle + \langle \psi^a \rangle \tag{1.4a}$$

$$= g^l \psi^l + g^s \psi^s + g^a \psi^a \tag{1.4b}$$

where volume fractions, g^ϕ, for each phase ϕ were used. Rappaz et al. [2003] define the volume fraction by writing a general expression inside the representative volume V_E:

$$g^\phi = \frac{1}{V_\mathrm{E}} \int_{V_\mathrm{E}} \chi^\phi(x,t)\, \mathrm{d}\Omega = \left\langle \chi^\phi \right\rangle \tag{1.5}$$

where the integrated quantity is an indicator (or presence) function relative to phase ϕ, which defines the volume of this phase in the system, Ω^ϕ, as follows:

$$\chi^\phi(x,t) = \begin{cases} 1 & \text{if } x \in \Omega^\phi \\ 0 & \text{otherwise} \end{cases} \tag{1.6}$$

Any phenomenon that may displace an interface, whether by phase change or a phase motion, is mathematically translated by variations of the presence function, such that its total derivative for each phase satisfies the following:

$$\frac{d\chi^\phi}{dt} = \frac{\partial \chi^\phi}{\partial t} + \vec{v^*} \cdot \vec{\nabla}\chi^\phi = 0 \tag{1.7}$$

If we consider the liquid phase, the variations of any quantity, named ψ, are given by:

$$\left\langle \frac{\partial \psi^l}{\partial t} \right\rangle = \frac{\partial \left\langle \psi^l \right\rangle}{\partial t} - \frac{1}{V_{\mathrm{E}}} \int_{l-a} \psi^l \overrightarrow{v^{l\text{-}a}} \cdot \overrightarrow{n^{l\text{-}a}} \, \mathrm{d}\Gamma - \frac{1}{V_{\mathrm{E}}} \int_{l-s} \psi^l \overrightarrow{v^{l\text{-}s}} \cdot \overrightarrow{n^{l\text{-}s}} \, \mathrm{d}\Gamma \tag{1.8}$$

$$\left\langle \vec{\nabla} \psi^l \right\rangle = \vec{\nabla} \left\langle \psi^l \right\rangle + \frac{1}{V_{\mathrm{E}}} \int_{l-a} \psi^l \overrightarrow{n^{l\text{-}a}} \, \mathrm{d}\Gamma + \frac{1}{V_{\mathrm{E}}} \int_{l-s} \psi^l \overrightarrow{n^{l\text{-}s}} \, \mathrm{d}\Gamma \tag{1.9}$$

$$\left\langle \vec{\nabla} \cdot \vec{\psi^l} \right\rangle = \vec{\nabla} \cdot \left\langle \vec{\psi^l} \right\rangle + \frac{1}{V_{\mathrm{E}}} \int_{l-a} \vec{\psi^l} \cdot \overrightarrow{n^{l\text{-}a}} \, \mathrm{d}\Gamma + \frac{1}{V_{\mathrm{E}}} \int_{l-s} \vec{\psi^l} \cdot \overrightarrow{n^{l\text{-}s}} \, \mathrm{d}\Gamma \tag{1.10}$$

Equation (1.7) can be recast with the level set method by using the smoothed Heaviside function in the metal. For the metal, this function is equal to one and decreases to zero in the air in a smooth way across both interfaces, solid-air and liquid-air. Since the solid phase is assumed fixed without possible deformation, and knowing that air is assumed incompressible, the solid-air interface does not move, leading to the following equation:

$$\frac{dH^M}{dt} = \frac{\partial H^M}{\partial t} + \overrightarrow{v^{l\text{-}a}} \cdot \vec{\nabla} H^M = 0 \tag{1.11}$$

1.4 FE model

In this section, we start from a the monodomain finite element model presented in **??** that was relevant to the metal only, referred to by the superscript M, then present the essential assumptions and formulations that allow predicting solidification shrinkage in a Eulerian context that introduces another domain, the air, referred to by the superscript A.

1.4.1 In the metal

Mass and momentum conservation

By assuming a fixed solid phase ($\vec{v^s} = \vec{0}$), the average velocity in the metal reduces only to liquid's average velocity. Therefore, we can write:

$$\langle \vec{v} \rangle^M = \left\langle \vec{v^l} \right\rangle = g^l \vec{v^l} \tag{1.12}$$

With eq. (1.12), the mass balance in the metal writes:

$$\frac{\partial \langle \rho \rangle^M}{\partial t} + \nabla \cdot \langle \rho \vec{v} \rangle^M = 0 \tag{1.13a}$$

$$\frac{\partial \langle \rho \rangle^M}{\partial t} + \nabla \cdot \left(g^l \rho^l \vec{v^l} \right) = 0 \tag{1.13b}$$

$$\frac{\partial \langle \rho \rangle^M}{\partial t} + \rho^l \nabla \cdot \left(g^l \vec{v^l} \right) + g^l \vec{v^l} \cdot \vec{\nabla} \rho^l = 0 \tag{1.13c}$$

$$\nabla \cdot \left\langle \vec{v^l} \right\rangle = -\frac{1}{\rho^l} \left(\frac{\partial \langle \rho \rangle^M}{\partial t} + \left\langle \vec{v^l} \right\rangle \cdot \vec{\nabla} \rho^l \right) \tag{1.13d}$$

Equation (1.13d) explains the flow due to shrinkage. A negative divergence term means that a liquid feeding is necessary to compensate for the density difference, hence acting as a flow driving force in the melt. Additional terms should appear in the other conservation equations, balancing the volume change in the heat and species transport.

When the metal's density was considered constant during solidification, the assumption of an incompressible system made it possible to use the Boussinesq approximation. However, in the case of solidification shrinkage, the average density $\langle \rho \rangle^M$ varies, as it depends on the solidification path as well as on ρ^s and ρ^l which are not equal nor constant. Therefore, the incompressibility condition may not be applicable. In such case, the earlier given system **??** is reformulated without any reference value for density:

$$\begin{cases} \rho^l \left(\dfrac{\partial \left\langle \vec{v^l} \right\rangle}{\partial t} + \dfrac{1}{g^l} \vec{\nabla} \cdot \left(\left\langle \vec{v^l} \right\rangle \times \left\langle \vec{v^l} \right\rangle \right) \right) = \\ - g^l \vec{\nabla} p^l - 2\mu^l \vec{\nabla} \cdot \left(\overline{\overline{\nabla}} \left\langle \vec{v^l} \right\rangle + \overline{\overline{\nabla}}^{\mathrm{t}} \left\langle \vec{v^l} \right\rangle \right) - g^l \mu^l \mathbb{K}^{-1} \left\langle \vec{v^l} \right\rangle + g^l \rho^l \vec{g} \\ \\ \nabla \cdot \left\langle \vec{v^l} \right\rangle = -\dfrac{1}{\rho^l} \left(\dfrac{\partial \langle \rho \rangle^M}{\partial t} + \left\langle \vec{v^l} \right\rangle \cdot \vec{\nabla} \rho^l \right) \end{cases} \tag{1.14}$$

Energy conservation

In the energy equation, a volumetric source term accounts for the heat dissipation caused by the shrinking metal volume. Before writing the new equation, we make the following assumptions:

- consequence of the static solid phase: $\langle \rho h \vec{v} \rangle = g^l \rho^l h^l \vec{v^l} + \cancel{g^s \rho^s h^s \vec{v^s}} = g^l \rho^l h^l \vec{v^l}$
- the heat generated by mechanical deformation, $\mathbb{S} : \dot{\varepsilon}$, is neglected

The unknowns in the energy conservation are the average volumetric enthalpy $\langle \rho h \rangle^M$ and temperature T. The energy conservation equation writes:

$$\frac{\partial \langle \rho h \rangle^M}{\partial t} + \nabla \cdot \langle \rho h \vec{v} \rangle^M = \nabla \cdot \left(\langle \kappa \rangle^M \vec{\nabla} T \right) \tag{1.15a}$$

$$\frac{\partial \langle \rho h \rangle^M}{\partial t} + \nabla \cdot \left(g^l \rho^l h^l \vec{v^l} \right) = \nabla \cdot \left(\langle \kappa \rangle^M \vec{\nabla} T \right) \tag{1.15b}$$

$$\frac{\partial \langle \rho h \rangle^M}{\partial t} + \left\langle \vec{v^l} \right\rangle \cdot \vec{\nabla} \left(\rho^l h^l \right) = \nabla \cdot \left(\langle \kappa \rangle^M \vec{\nabla} T \right) - \rho^l h^l \nabla \cdot \left\langle \vec{v^l} \right\rangle \tag{1.15c}$$

$$\frac{\partial \langle \rho h \rangle^M}{\partial t} + \left\langle \vec{v^l} \right\rangle \cdot \vec{\nabla} \left(\rho^l h^l \right) = \nabla \cdot \left(\langle \kappa \rangle^M \vec{\nabla} T \right) + h^l \left(\frac{\partial \langle \rho \rangle^M}{\partial t} + \left\langle \vec{v^l} \right\rangle \cdot \vec{\nabla} \rho^l \right) \tag{1.15d}$$

The second term in the RHS of eq. (1.15d) is a heat power (of unit $W m^{-3}$) that adds to the system in the mushy zone. This term is proportional to the solidification rate and expresses the heat generated in regions where the average density is changing and/or a gradient of liquid density is being advected.

Species conservation

The last conservation principle is applied to the chemical species or solutes. This principle allows predicting macrosegregation when applied to a solidification system, along with the mass, momentum and energy balances. However, the conservation equation should be reformulated in the case of a melt flow driven by shrinkage. Assumptions

- the solidification path is tabulated using thermodynamic data at equilibrium
- the macroscopic solute diffusion coefficient D^s in the solid phase is neglected in the mass diffusive flux term.
- consequence of the static solid phase: $\langle \rho w \vec{v} \rangle^M = g^l \rho^l \langle w \rangle^l \vec{v^l} + \cancel{g^s \rho^s \langle w \rangle^s \vec{v^s}} = g^l \rho^l \langle w \rangle^l \vec{v^l}$

The species conservation is pretty similar the energy conservation formulated in the previous section. The main difference is the breakup of the volumetric variable $\langle \rho w \rangle^M$ into a product of density $\langle \rho \rangle^M$ and the mass concentration $\langle w \rangle^M$. For a binary alloy, we write:

$$\frac{\partial \langle \rho w \rangle^M}{\partial t} + \nabla \cdot \langle \rho w \vec{v} \rangle^M - \nabla \cdot \left(\left\langle D^l \right\rangle \vec{\nabla} \left(\rho^l \langle w \rangle^l \right) \right) = 0 \tag{1.16a}$$

$$\langle \rho \rangle^M \frac{\partial \langle w \rangle^M}{\partial t} + \langle w \rangle^M \frac{\partial \langle \rho \rangle^M}{\partial t} + \nabla \cdot \left(g^l \rho^l \langle w \rangle^l \vec{v^l} \right) - \nabla \cdot \left(g^l D^l \vec{\nabla} \left(\rho^l \langle w \rangle^l \right) \right) = 0 \tag{1.16b}$$

$$\begin{aligned} &\langle \rho \rangle^M \frac{\partial \langle w \rangle^M}{\partial t} + \langle w \rangle^M \frac{\partial \langle \rho \rangle^M}{\partial t} + \left(\rho^l \langle w \rangle^l \right) \nabla \cdot \left\langle \vec{v^l} \right\rangle + \left\langle \vec{v^l} \right\rangle \cdot \vec{\nabla} \left(\rho^l \langle w \rangle^l \right) \\ &- \nabla \cdot \left(g^l D^l \vec{\nabla} \left(\rho^l \langle w \rangle^l \right) \right) = 0 \end{aligned} \tag{1.16c}$$

The mass balance gives the following relation when the liquid density is constant:

$$\nabla \cdot \left\langle \vec{v^l} \right\rangle = -\frac{1}{\rho^l} \left(\frac{\partial \langle \rho \rangle^M}{\partial t} \right) \tag{1.17}$$

If we use the result of eq. (1.17) in eq. (1.16c), then we get the following equation:

$$\langle \rho \rangle^M \frac{\partial \langle w \rangle^M}{\partial t} + \langle w \rangle^M \frac{\partial \langle \rho \rangle^M}{\partial t} = \langle w \rangle^l \frac{\partial \langle \rho \rangle^M}{\partial t} - \left\langle \vec{v^l} \right\rangle \cdot \vec{\nabla} \left(\rho^l \langle w \rangle^l \right) + \nabla \cdot \left(g^l D^l \vec{\nabla} \left(\rho^l \langle w \rangle^l \right) \right) \tag{1.18}$$

Applying Voller-Prakash [Voller et al. 1989] variable splitting, the system ends up with only one variable, $\langle w \rangle^M$. The splitting is done as follows:

$$\langle w \rangle^l = \left(\langle w \rangle^l \right)^t + \langle w \rangle^M - \left(\langle w \rangle^M \right)^t \tag{1.19}$$

where the superscript t refers to the previous time step. The chemical species conservation writes:

$$\begin{aligned} &\langle \rho \rangle^M \frac{\partial \langle w \rangle^M}{\partial t} + \cancel{\langle w \rangle^M \frac{\partial \langle \rho \rangle^M}{\partial t}} = \\ &\cancel{\langle w \rangle^M \frac{\partial \langle \rho \rangle^M}{\partial t}} - \rho^l \left\langle \vec{v^l} \right\rangle \cdot \vec{\nabla} \langle w \rangle^M + \nabla \cdot \left(g^l \rho^l D^l \vec{\nabla} \langle w \rangle^M \right) \\ &+ \frac{\partial \langle \rho \rangle^M}{\partial t} \left[\left(\langle w \rangle^l \right)^t - \left(\langle w \rangle^M \right)^t \right] - \rho^l \left\langle \vec{v^l} \right\rangle \cdot \vec{\nabla} \left(\left(\langle w \rangle^M \right)^t - \left(\langle w \rangle^l \right)^t \right) \end{aligned} \tag{1.20a}$$

$$\begin{aligned} &\langle \rho \rangle^M \frac{\partial \langle w \rangle^M}{\partial t} + \rho^l \left\langle \vec{v^l} \right\rangle \cdot \vec{\nabla} \langle w \rangle^M - \nabla \cdot \left(g^l \rho^l D^l \vec{\nabla} \langle w \rangle^M \right) = \\ &- \frac{\partial \langle \rho \rangle^M}{\partial t} \left[\left(\langle w \rangle^M \right)^t - \left(\langle w \rangle^l \right)^t \right] + \rho^l \left\langle \vec{v^l} \right\rangle \cdot \vec{\nabla} \left(\left(\langle w \rangle^M \right)^t - \left(\langle w \rangle^l \right)^t \right) \\ &- \nabla \cdot \left[g^l \rho^l D^l \vec{\nabla} \left(\left(\langle w \rangle^M \right)^t - \left(\langle w \rangle^l \right)^t \right) \right] \end{aligned} \tag{1.20b}$$

$$\begin{aligned}
&\langle \rho \rangle \frac{\partial \langle w \rangle^M}{\partial t} + \rho^l \left\langle \vec{v^l} \right\rangle \cdot \vec{\nabla} \langle w \rangle^M - \nabla \cdot \left(g^l \rho^l D^l \vec{\nabla} \langle w \rangle^M \right) = \\
&- \frac{\partial \langle \rho \rangle^M}{\partial t} \left[\left(\langle w \rangle^M \right)^t - \left(\langle w \rangle^l \right)^t \right] \\
&+ \rho^l \left\langle \vec{v^l} \right\rangle \cdot \vec{\nabla} \left(\left(\langle w \rangle^M \right)^t - \left(\langle w \rangle^l \right)^t \right) - \nabla \cdot \left[g^l \rho^l D^l \vec{\nabla} \left(\left(\langle w \rangle^M \right)^t - \left(\langle w \rangle^l \right)^t \right) \right]
\end{aligned} \tag{1.21}$$

It is noted that eq. (1.21) is valid only if both densities ρ^l and ρ^s are constant but have different values. Since density changes are incorporated in this equation, inverse segregation following solidification shrinkage is predicted. For the case where macrosegregation is solely due to fluid flow generated by natural or forced convection, i.e. no shrinkage occurs whether due to thermal-solutal contraction or phase change, the overall volume remains constant, hence density is constant. In this situation, $\rho^s = \rho^l = \langle \rho \rangle$ and the term $\partial \langle \rho \rangle / \partial t$ therefore vanishes. After dividing both sides by $\langle \rho \rangle = \rho^l$, eq. (1.21) reduces to:

$$\begin{aligned}
&\frac{\partial \langle w \rangle^M}{\partial t} + \left\langle \vec{v^l} \right\rangle \cdot \vec{\nabla} \langle w \rangle^M - \nabla \cdot \left(g^l D^l \vec{\nabla} \langle w \rangle^M \right) \\
&= \left\langle \vec{v^l} \right\rangle \cdot \vec{\nabla} \left(\left(\langle w \rangle^M \right)^t - \left(\langle w \rangle^l \right)^t \right) - \nabla \cdot \left[g^l D^l \vec{\nabla} \left(\left(\langle w \rangle^M \right)^t - \left(\langle w \rangle^l \right)^t \right) \right]
\end{aligned} \tag{1.22}$$

1.4.2 In the air

The presence of an air domain in our approach is important to follow the free surface of the solidifying metal. For this particular reason, some assumptions are introduced and explained in this section in order to limit unnecessary treatment within the air, since it does not undergo phase change. It should be reminded that we consider air as a single-phase system, hence superscripts A and a are interchangeably used.

Mass and momentum conservation

To simplify fluid flow resolution in the air, we consider it as incompressible. This assumption is acceptable in the context of casting processes where air velocity has an insignificant order of magnitude. Therefore, the free metal surface is not disturbed by air flow in its vicinity. With the incompressibility of air, we are saying that any deformation of the free surface is solely due to an air mass increase, coming from the system boundaries. The mass balance hence writes:

$$\nabla \cdot \langle \vec{v} \rangle^A = \nabla \cdot \vec{v^a} = 0 \tag{1.23}$$

The air flow is governed by time-dependent incompressible Navier-Stokes equations, as previously done for the metal:

$$\begin{cases} \rho^a \left(\dfrac{\partial \vec{v^a}}{\partial t} + \vec{\nabla} \cdot \left(\vec{v^a} \times \vec{v^a} \right) \right) = \\ -\vec{\nabla} p^a - 2\mu^a \vec{\nabla} \cdot \left(\overline{\overline{\nabla}} \vec{v^a} + \overline{\overline{\nabla}}^{\mathrm{t}} \vec{v^a} \right) + \rho^a \vec{g} \\ \\ \nabla \cdot \vec{v^a} = 0 \end{cases} \tag{1.24}$$

The air density ρ^a is considered constant along the casting process, therefore thermal gradients in the air that arise due to the low thermal conductivity, do not generate any flow, i.e. no Boussinesq approximation is made on the term $\rho^a \vec{g}$ in eq. (1.24).

Energy conservation

It was mentioned in the introduction of the current section that air is a single-phase system that cannot undergo any phase change. Therefore, heat transfer in this domain simplifies to pure thermal conduction with a low thermal conductivity coefficient, $\langle\kappa\rangle^a$. The energy balance in the governs the air enthalpy $\langle\rho h\rangle^A$ (which is equal to $\rho^a h^a$ in the current context) as follows:

$$\frac{\partial \langle \rho h \rangle^A}{\partial t} + \nabla \cdot \langle \rho h \vec{v} \rangle^A = \nabla \cdot \left(\langle \kappa \rangle^A \vec{\nabla} T \right) \tag{1.25a}$$

$$\frac{\partial \langle \rho h \rangle^A}{\partial t} + \nabla \cdot \left(\rho^a h^a \vec{v^a} \right) = \nabla \cdot \left(\langle \kappa \rangle^a \vec{\nabla} T \right) \tag{1.25b}$$

$$\frac{\partial \langle \rho h \rangle^A}{\partial t} + \vec{v^a} \cdot \vec{\nabla} \left(\rho^a h^a \right) = \nabla \cdot \left(\langle \kappa \rangle^a \vec{\nabla} T \right) \tag{1.25c}$$

Species conservation

The composition of alloying elements is crucial quantity to predict in this work. Nevertheless, such prediction is only relevant in the metallic alloy, even if the air is also made up of other chemical species (nitrogen, oxygen ...). For this obvious reason, the species conservation equation should not be solved in the air, but that of course is contradictory to the monolithic resolution. The consequence is that we should compute the conservation of chemical species in the air and the metal, but limit as much as possible the influence of the former, in a way to prevent a "numerical" solute exchange between these domains. To do so, the computed air velocity will not be used here for advection, but rather use a zero-velocity vector instead. As diffusion is also another transport mechanism that may alter the conservation principle, a very low macroscopic solute diffusion coefficient can be used, as long as its order of magnitude is at most a thousand times less than that in the melt, $D^a \lll D^l$. The low artificial diffusion in the air may slightly violate the wanted no-exchange condition at the air-liquid interface, but it is known that suppressing the diffusion term in the air would result in a numerically stiff partial differential equation.

$$\frac{\partial}{\partial t}\left(\rho^a \langle w \rangle^A\right) + \cancel{\nabla \cdot \left(\rho^a \langle w \rangle^A \left\langle \vec{v^a} \right\rangle\right)} - \nabla \cdot \left(\rho^a D^a \vec{\nabla} \langle w \rangle^A\right) = 0 \tag{1.26}$$

$$\boxed{\frac{\partial}{\partial t}\left(\rho^a \langle w \rangle^A\right) - \nabla \cdot \left(\rho^a D^a \vec{\nabla} \langle w \rangle^A\right) = 0} \tag{1.27}$$

1.5 FE monolithic model

The monolithic model combines all conservations equations in metal and air in a unique set of equations to be solved on a fixed mesh. This can be accomplished by using the Heaviside function (defined in **??**) relative to each domain.

1.5.1 Permeability mixing

How to mix liquid fraction, best using harmonic or arithmetic, in order to replicate the effect the of non slip condition at top for example
Put the python plots from the presentations in "TEXUS monolithic"
Put video animations of PSEUDO SMACS 2D without and with LS ???

1.5.2 Model equations

Rewrite air-metal monolithic conservation equations using mixture laws.

1.5.3 Interface treatment

The level set method, like any other interface tracking/capturing method, needs defining a convenient way of coupling the velocity field on the one hand, which is the solution provided by solving momentum conservation equations, with the interface position on the other hand. The question is "how does the velocity field transport the interface?". The answer is potentially one of two possibilities: classical coupling or modified coupling. In the next subsections, we discuss the technical details of each approach and the hurdles that come with it.

Classical coupling

A "classical" coupling comes in the sense of "unmodified" coupling. This approach consists of taking the output of the fluid mechanics solver, then feed it as raw input to level set transport solver. The physical translation would be that the interface motion is dictated by the fluids flow in its vicinity. No treatment whatsoever is done between the two mentioned steps. While conservation principles are best satisfied with this approach, the latter yields some drawbacks, preventing its application in a generic way. For instance, the free liquid surface is not necessarily horizontal at all times and that can lead to the wrong shrinkage profile when solidification is complete.

present the example of unstable interface when the ratio between fluids properties became greater than some value+discussion

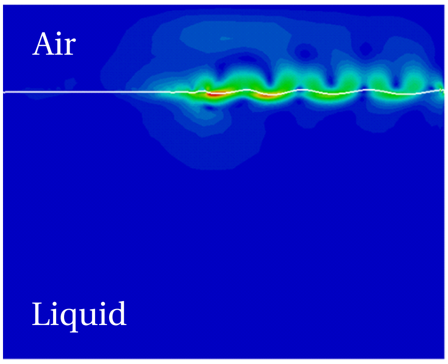

(a) At a certain time increment (without mesh)

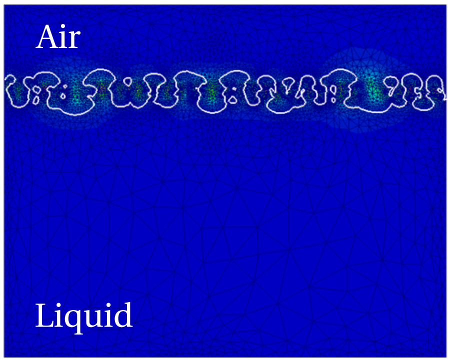

(b) Another time increment (with mesh)

Fig. 1.4 – Interface destabilisation under the effect of high properties ratio across the interface.

Modified coupling

In contrast to a classic coupling, here we attempt to modify the velocity field before feeding to the transport solver. The main motivation for considering this approach is the lack of stability that we observed whenever the mechanical properties of the fluids were different by several orders of magnitude. The algorithm should simultaneously fulfil these requirements:

- support high ratios of fluids density with close viscosities by preserving an non-oscillating interface,
- maintain a horizontal level at the free surface of the melt,
- follow shrinking metal surface profile in solidfying regions,
- satisfy the mass conservation principle, essentially in the metal.

We want to process the original transport velocity by imposing a uniform motion (speed and direction) at the nodes of the free surface, and at the same time, be able to follow the pipe formation at the surface as a result of solidification shrinkage, as shown in fig. 1.5.

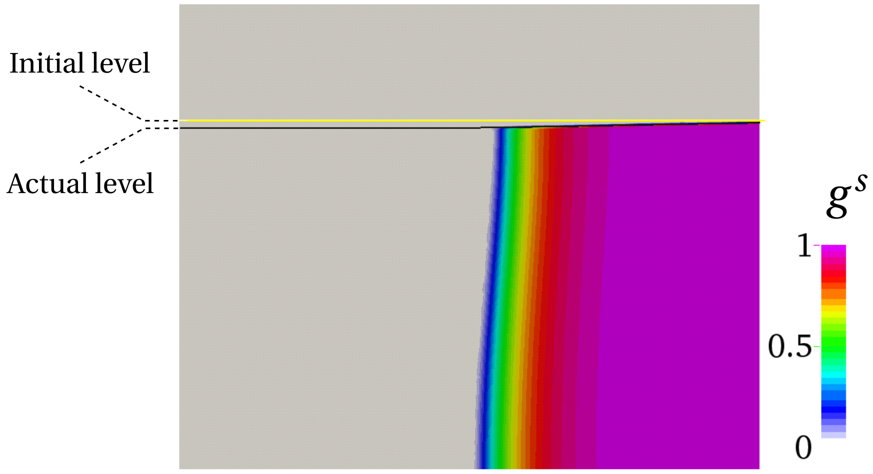

Fig. 1.5 – Snapshot of a solidifying ingot by a cooling flux from the side. The profile of the actual surface changes in solid and mushy regions to adapt the new density while staying perfectly horizontal in the liquid phase.

How to transport level set using velocity from momentum conservation DIRECTLY or AVERAGED PER ELEMENTS, show examples of instability/stability when using false/nominal air properties
Validation of LS transport: perform test case simulation of buoyancy driven air droplet in water by 2005Nagrath that I also have seen in Shyamprasad's masters report). => I didnt notice: what time step δt did they use ?

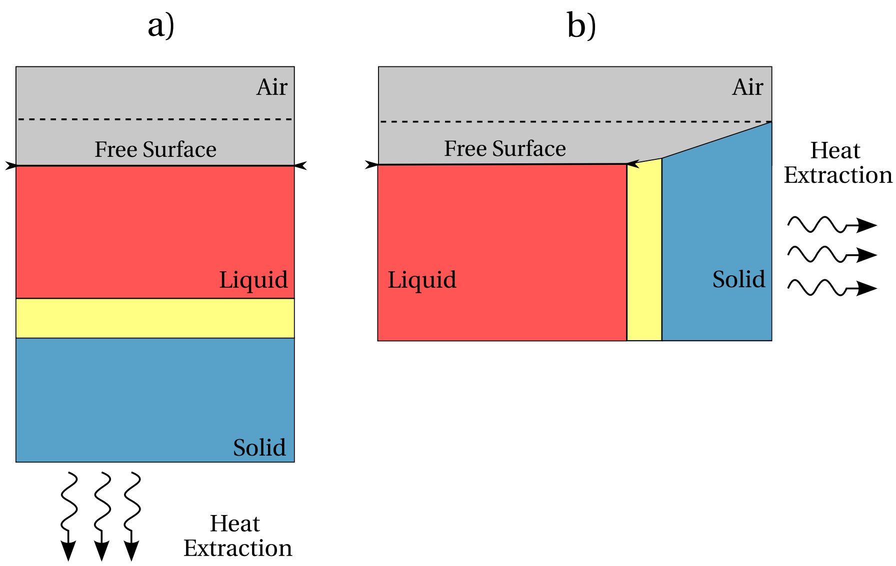

Fig. 1.6 – Treatment of liquid free surface in a) bottom and b) side heat extraction configurations. The dashed line represents the initial level of the free liquid surface.

The general idea is read the velocity around the interface up to a certain thickness, which may be the same thickness as the diffuse interface defined in **??**, then compute a volumetric average from all the elements in the thickness. This average is then given to the transport solver, which will apply the same magnitude and direction to transport the interface. However, as we only need the transport velocity to be uniform within the "100% liquid" elements, it should not be the case for the other elements that belong either to the mushy zone or the solid region, where shrinkage is taking place. Therefore, depending on the heat extraction configuration, two scenarios are possible. If heat extraction is far from the interface, i.e. there is not direct contact as in fig. 1.6a, the surface area remains unchanged at any time, hence all the elements around the interface are "100% liquid". This happens when a bottom cooling is applied to the ingot. In contrast, if a side cooling is applied as shown in fig. 1.6b, the surface area of the interface will be reduced over time as a consequence of the solid front progression. In this case, the average transport velocity should be computed only from the elements belonging to the free surface. The remaining part of the interface which belongs to partial or full solid regions, is transported with Navier-Stokes output, which should be some orders of magnitude less than the velocity imposed at the free surface, as a result of a decreasing permeability.

1.6 Shrinkage without macrosegregation

Explain how the flow and heat transfer in the air are not important
Give the strong form equations to be solved OR simply refer the previous section where the model was defined
Initial and boundary conditions for energy and momentum: Initially we have liquid and air at rest.

1.6.1 Al-7wt% Si

Present pseudo 1D case with results + discussion

1.6.2 Pb-3wt% Sn

Present 2D and 3D case with results + discussion

1.7 Shrinkage with macrosegregation

Explain how the flow and heat transfer in the air are not important
Give the strong form equations to be solved OR simply refer the previous section where the model was defined
Initial and boundary conditions for energy and momentum: Initially we have liquid and air at rest.

1.7.1 Al-7wt% Si

Present pseudo 1D case with results + discussion

1.7.2 Pb-3wt% Sn

Present 2D and 3D case with results + discussion

Bibliography

[Onodera et al. 1959]

Onodera, S. and Arakida, Y. (1959). "Effect of Gravity on the Macro-Segregation of Larger Steel Ingots", pp. 358–368. URL: http://eprints.nmlindia.org/3079/1/358-368.PDF (cited on page 3).

[Rappaz et al. 2003]

Rappaz, M., Bellet, M., and Deville, M. (2003). *Numerical Modeling in Materials Science and Engineering*. Springer Series in Computational Mathematics. Springer Berlin Heidelberg (cited on page 5).

[Voller et al. 1989]

Voller, V. R., Brent, A. D., and Prakash, C. (1989). "The modelling of heat, mass and solute transport in solidification systems". *International Journal of Heat and Mass Transfer*, 32 (9), pp. 1719–1731. URL: http://www.sciencedirect.com/science/article/pii/0017931089900549 (cited on page 9).